PCCP

Supersonic Jet Chirped Pulse Microwave Spectroscopy of Ring-Like Methanol:Water Pentamers

Journal:	*Physical Chemistry Chemical Physics*
Manuscript ID	CP-ART-06-2023-003005.R1
Article Type:	Paper
Date Submitted by the Author:	18-Sep-2023
Complete List of Authors:	Mastin, Evan; California Institute of Technology, Chemistry Dutton, Sarah; California Institute of Technology, Chemistry Blake, Geoffrey; California Institute of Technology, Division of Geology and Planetary Science; California Institute of Technology, Division of Chemistry and Chemical Engineering

PCCP

ARTICLE TYPE

Cite this: DOI: 00.0000/xxxxxxxxxx

Supersonic Jet Chirped Pulse Microwave Spectroscopy of Ring-Like Methanol:Water Pentamers†

E.M. Mastin,* S.E. Dutton,* and G.A. Blake*

Received Date
Accepted Date

DOI: 00.0000/xxxxxxxxxx

The potential energy surfaces of pure methanol and mixed methanol-water pentamers have been explored using chirped pulse Fourier-transform microwave spectroscopy aided by *ab initio* calculations. Rotational constants, anharmonic corrections, dipole moments, and relative energies were calculated for different conformers. Predicted rotational transitions were then fit to experimental spectra from 10 – 18 GHz and the assignments were confirmed using double resonance experiments where feasible. The results show all 23 of the lowest energy conformers are bound in a planar ring of hydrogen bonding that display a steady decrease in the R_{O-O} distance along this ring as methanol content is increased. Interspersed methanol and water conformers have comparable relative abundances to those with micro-aggregation, but structures with micro-aggregated methanol and water have a higher rigid rotor fitting error. The computational methods' high degree of accuracy when compared to our experimental results suggests the strong donor-acceptor hydrogen bonding in these clusters leads to well-defined minima on the intermolecular potential energy surface.

1 Introduction

Hydrogen bonding is extensively studied due to the vital role it plays in many fields of science. For example, in biology, H-bonds are needed to maintain protein structure(s) and to drive DNA base-pairing and stability[1,2]. Further, formation of molecular complexes in the atmosphere are often driven by H-bonding interactions[3], while solvent-solute interactions and molecular solvation can be dictated by H-bonding. Yet, given its importance and the breadth of previous research, open questions regarding the energetics and structure of H-bonding in small clusters remain[4]. Specifically, the H-bonding characteristics of methanol-water clusters lack the direct, high precision structural information that rotational spectroscopy can provide[5].

Using molecular clusters as a tool to study H-bonding can provide clarity to theoretical work aiming to model bulk properties of the molecule(s)[6]. For this reason, large cluster studies have been performed with benzaldehyde-water[7], glycoaldehyde-water[8], phenol-water[9], benzyl alcohol-water[10], and more. Previous work even investigates similar methanol-water clusters[11–14], but using techniques that infer, rather than accurately measure, the structures of the clusters.

Methanol is an ideal model for studying small H-bonding clusters, being the simplest organic molecule capable of forming H-bonds with water and itself[15]. Methanol and water can both act as H-bond donors and acceptors, but where water has two donor and two acceptor sites, the methyl group in CH_3OH means it has only one donor site and up to two acceptor sites[16]. To investigate the interplay of these properties, we have performed conformational studies of methanol and water clusters. Pentamers, both pure and mixed, are the largest clusters which have geometries and cooperativity unaffected by the difference in donor/acceptor sites. That is, each pentamer conformer studied here is planar with a net cooperativity of two.

It would be difficult to overstate the importance of water, but methanol is also one of the most common solvents; it is the most abundant oxygenated volatile organic compound in the atmosphere[17], an attractive clean fuel alternative and chemical feed stock[18–20], and an important regulatory molecule in the human body[21,22]. Yet it remains a challenge to comprehensively model methanol and methanol-water systems. Precise information on H-bonded cluster geometries provided by rotational spectroscopy can help improve the accuracy of bulk models based on intermolecular interactions. The Blake group Chirped Pulse Fourier-Transform Microwave (CPFTMW) spectrometer, described previously[23], is especially suited for the characterization of the larger clusters that may inform more representative models of liquids and mixtures. The spectrometer is fit with a high throughput, high compression ratio turbomolecular pump, allowing for continuous expansion of sample clusters. The high duty cycle thus enabled allows for extensive, efficient averaging. The weak transitions in the dense spectra of mixed vapors that we are studying here are only attainable with the sensitivity provided by consid-

*Division of Chemistry and Chemical Engineering, California Institute of Technology, 1200 E California Blvd., Pasadena, CA 91125, USA. E-mail: gab@gps.caltech.edu

† Electronic Supplementary Information (ESI) available: [details of any supplementary information available should be included here]. See DOI: 10.1039/cXCP00000x/

erable averaging.

In this article, pure methanol and mixed methanol-water pentamers are studied as an extension from previous computational and experimental work on dimers[24], trimers[25,26], and tetramers[15]. The Blake group has previously examined ethanol-water dimers[27], trimers[23], and tetramers[28]. However, methanol is used here instead of ethanol, since its higher vapor pressure leads to the facile formation of large clusters. In addition, methanol's simplified geometry (especially the lack of gauche vs. trans conformations in the ethyl group) significantly decreases the number of conformer permutations and associated computational cost. In total, 23 of the lowest energy conformers were observed and assigned.

2 Methods

2.1 Computational

To keep track of the many conformers, a shorthand naming convention is used. Each structure has a ring of H-bonding with methyl groups lying above or below the plane of H-bonding, where the ambiguous "above or below" the plane is distinguished by the right-hand screw rule with respect to the ring of H-bonds. To denote a methyl group that is above the H-bond plane, an upward arrow (pictorially) or "u" (in text) is used; to denote a methyl group that is below the plane, a "d" or downward arrow is used. A simplistic picture of the pure methanol pentamer, with its shorthand name and full structure, can be referenced in Figure 1. The naming convention for the pure methanol pentamer, from the top methanol following the H-bonds counterclockwise, yields uduud for methyl groups above, below, above, above, and below the plane of H-bonding, respectively. Water is always labeled "w," whether water's free hydrogen is above or below the plane. The only instance where the lack of a water label is insufficient in distinguishing conformers is the case of the two wwwwd conformers. Here, wwwwd has alternating hydrogen positions and wwwwd′ has hydrogens up, down, down, up.

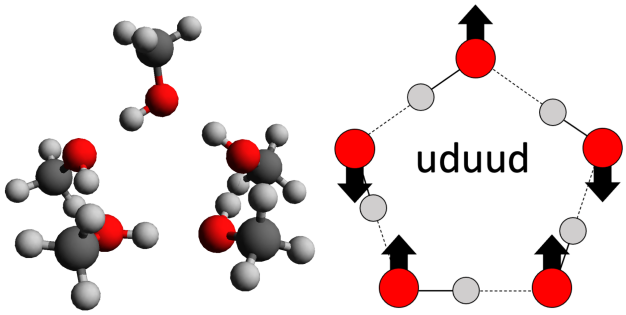

Fig. 1 Full structure of the methanol pentamer, viewed from slightly above the plane of H-bonding on the left, with the associated simple depiction and naming convention on the right.

Although not explicitly defined in the naming scheme, water's free hydrogen becomes important as water content increases. With only one water or two water molecules in the cluster, the free hydrogen in a water molecule appears to be locked in place due to the high barrier of flipping while next to a methyl group. However, in micro-aggregated three water clusters, it is possible to have a water that is not adjacent to a methyl group on either side. In this case, under the right circumstances, the barrier to flipping a single hydrogen is low enough to not form a distinct conformer, but rather averages out the structure on rotational time scales. An example of the one conformer in which this is observed is given in Figure 2.

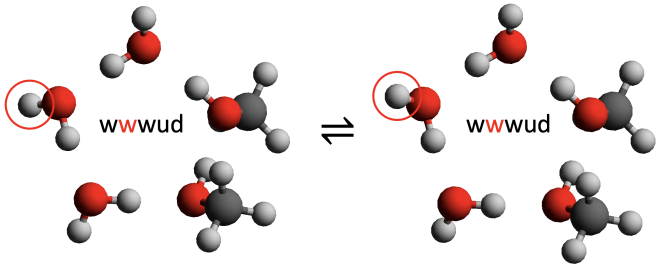

Fig. 2 A free hydrogen flipping from below to above the plane of hydrogen bonding. This motion is accessible since the hydrogen is adjacent to two waters.

Conformers consistent with the ring motif described above were assembled by hand rather than a sampling program using force fields. Detailed structures of these lowest energy methanol-water pentamers were then optimized with `Gaussian 16`[29]. Optimized geometries, rotational constants, quartic centrifugal distortion corrections, dipole moments, and free energies were calculated at the density functional B3LYP level of theory using the 6–311++G(d,p) basis set. This level of theory and basis set combination has been shown to be sufficient in previous work[15,25,28], and the associated moderate computational cost was desirable when calculating the copious pentamer conformers. Upon convergence of each calculation, rotational constants and anharmonic corrections were used to create simulated line lists with `PGOPHER`[30] and `SPCAT`[31] for comparison to experiment.

For every methanol in each cluster, splitting of the rotational states due to internal rotation of the methyl rotor had to be considered. Barrier heights to methyl rotations were calculated with B3LYP/6–311++G(d,p), and these barrier heights were used to find the magnitude of splitting with `XIAM`[32]. In contrast to previous work with ethanol where the splittings were small enough to only increase error in the experimental line position(s), here the internal rotor splittings were readily resolvable, on the order of 100 MHz. Ideally, this meant we could fit to both A and E state rotational transitions. However, with clusters having up to five distinct methyl rotors, these large clusters are beyond available internal rotation fitting methods, and so to make initial assignments we approximated some methyl rotors as having the same environment and reducing to two 'types' of rotors. This method made it obvious the transitions would still be resolvable, but could not yield sufficiently precise non-A-A predicted splittings for assignment and fitting, given the high line density in the planar expansion. Since this approximation was necessary for only some of the conformers, for consistency we exclusively fit only A-A transitions for all conformers.

2.2 Experimental

The CPFTMW spectrometer has been previously described[23], so only a brief overview of the current experiments are provided here.

The efficient formation of pentamers required a backing pressure of 3 atm Argon bubbling through methanol first, then through water in a separate bubbler. The water was heated to 60 °C, the point at which its vapor pressure is roughly equivalent to methanol's at room temperature. When forming pure methanol clusters, water was taken off line and methanol was heated to 60 °C. Flow into the chamber was regulated to 50 sccm through a mass flow controller and the pressure was kept at roughly 3×10^{-4} Torr while the clusters underwent a continuous supersonic expansion through a 5.7 cm × 25 μm slit nozzle.

The chirp used in this experiment is 1.2 μs long with a repetition rate of 25 kHz and spans DC to 2 GHz (effectively 190 to 1,820 MHz). The chirp is heterodyned with a local oscillator (LO) allowing for frequencies up to 18 GHz to be studied. The measurement is dual side-band, so one LO setting covers roughly 4 GHz. At each LO setting, 200 million 18 μs free induction decay acquisitions were averaged. The non-deuterated spectra covers 10.0 – 17.8 GHz, the perdeuterated methanol spectra covers 10.2 – 18.3 GHz, and the D_2O spectra spans 10.2 – 18.0 GHz. The non-deuterated and perdeuterated methanol spectra are an average of 10 LO settings, or 2 billion acquisitions, while the D_2O spectrum is an average of 6 LO settings, or 1.2 billion acquisitions. Fewer LO settings were taken with D_2O reducing sample consumption and resulting in decreased spectral overlap between separate LO acquisitions.

3 Results and Discussion

The 23 normal isotopologue pentamer conformers for which rotational constants, anharmonic corrections, dipole moment, and energies have been calculated are depicted in Figure 3. The *A*, *B*, and *C* rotational constants were well fit for each conformer. Distortion corrections were fit when possible, but otherwise were fixed to their computed values, as described below. Fitting was performed with `SPFIT`[31] using the A or S reduction of Watson's Hamiltonian in the I^r representation. The absolute values for Ray's asymmetry parameter range from 0.003 (wuduu) to 0.93 (uduud), so the strongest fitting reduction was chosen, but kept consistent, for each hydration level.

Table 1 represents the singular minimum for the pure methanol pentamer. Its inverse conformer, duddu, has the same calculated rotational constants thus we believe it is the same structure. Other permutations of u and d methyl groups either default to uduud/duddu by cycling the starting point of the naming convention or place more than two adjacent methyl groups on the same side of the H-bonding plane. This excessive crowding of the methyl groups on the same side of the plane results in much higher energy, and these structures are therefore not included in our analysis.

With the addition of one water to the cluster, we found five minima within 55 cm^{-1} of each other, (see Table 2). As with the pure methanol pentamer, any permutation outside of these five either completely flips the cluster and returns to the same geometry or results in an energetically unfavorable crowding of adjacent methyl groups.

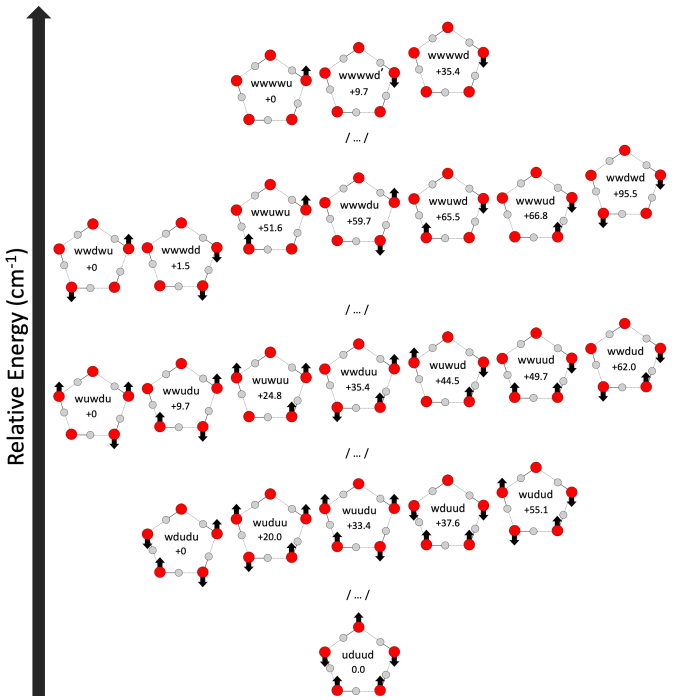

Fig. 3 Pentamer conformers ordered by relative energies within each hydration level. Each replacement of methanol with water leads to a roughly 6,500 cm^{-1} (~18.5 kcal/mol) increase in energy.

Pentamers containing two and three water molecules, summarized in Tables 3 and 4, respectively, have seven minima each. One conformer for the three water clusters, wwwud, did not have enough observed lines to fit *any* of the quartic distortion constants. In the case of wwwud, the free hydrogen that lies between the two waters is able to flip above and below the plane of hydrogen bonding with little resistance. The facile proton motion leads to the averaging of two similar geometries increasing the difficulty in assignments. More generally for two and three water clusters, the decrease in observable transitions may be linked to lower abundance, which in turn could be attributed to the fact that as more conformers per hydration level became energetically available, population, and thus intensity, is spread between them.

Further, our computational results show that for the mixed pentamers, in which the methyl groups in CH_3OH do not 'cost' any hydrogen bond interactions since all monomers have a cooperativity of two, those with higher water content are commensurately higher in energy – thus helping to explain the difficulty in observing these high water content clusters. Such pentamers also have, on average, lower S/N, and as a result are more challenging to fit. This is also thanks to the low vapor pressure of water relative to methanol, which leads to methanol-favored clusters under expansion conditions.

To round out the survey of the mixed methanol and water pentamer potential energy space, three pentamer conformers with four water and one methanol were observed. Compared to two and three water clusters, intensity was only spread between three conformers rather than seven and only one methyl rotor created

uduud	Ab Initio	Fitted
A /MHz	675.396	675.512 (11)
B /MHz	665.306	665.220 (11)
C /MHz	400.555	400.325 (40)
Δ_J /kHz	0.31	0.28 (3)
Δ_K /kHz	0.25	1.54 (21)
Δ_{JK} /kHz	-0.43	-2.14 (27)
δ_J /kHz	-0.0023	-0.0023
δ_K /kHz	0.049	0.049
μ_a /D	-0.29	y
μ_b /D	0.11	n
μ_c /D	0.64	y
N	–	13
rms /kHz	–	64

Table 1 Calculated and experimental rotational constants for the pure methanol pentamer. Parameters are fit *via* SPFIT, using Watson's S-reduction of the Hamiltonian. N is the number of lines from the experimental spectrum fit, and the values in parentheses are the errors reported by SPFIT. Experimental parameters shown without error were fixed to the computed values for fitting.

internal rotation splitting. The results of fitting the rotational states for these species are shown in Table 5. The individual water monomer free hydrogen for both wwwwu and wwwwd alternate around the ring, but for wwwwd′, the hydrogens are above the plane when adjacent to the down methyl group and both below the plane otherwise. It should be noted that the pure water pentamer is not observed due to its rotationally averaged symmetry (that is, lack of a permanent dipole moment), caused by the facile pseudo-rotation of the OH bonds in this species, as is also the case in the pure water trimer[33].

In the present work, the agreement between predicted rotational constants and experimentally derived rotational constants is extremely good, with a difference in the primary rotational constants typically less than a megahertz. This may be explained by the strong, and coupled, donor-acceptor hydrogen bonding in the clusters, in that this stability leads to well-defined minima on the potential energy surface. These well-defined minima, even in the presence of many conformers for a given cluster composition, are thus in turn well described by the DFT methods used herein. Due to the limited range of J and K rotational states per fit, arising from the modest frequency coverage and low excitation temperature, and the S/N achieved in these large clusters, robust determination of the distortion constants was challenging. Thus, when prudent, the highest order distortion constants were left fixed to computed values, especially when unphysical results were returned by SPFIT[34]. Additionally, the presence of low lying intermolecular vibrational modes for each conformer can lead to extensive anharmonic structural averaging even in the ground state, further hindering the accurate assignment of a full suite of distortion constant. The emphasis of this work is therefore centered on the structural constraints that are derived from the accurately determined A, B, and C rotational constants.

Figure 4 displays a section of the 8 GHz experimental spectrum with non-deuterated methanol and water. This section of the spectrum has a sample of each hydration level besides pure methanol (which was assigned from features in a pure Ar:Methanol expansion). After fitting a spectrum, dual resonance experiments were performed when possible to confirm the assignments of the lines listed. Confirmed dual resonance connections are shown in the ESI.†

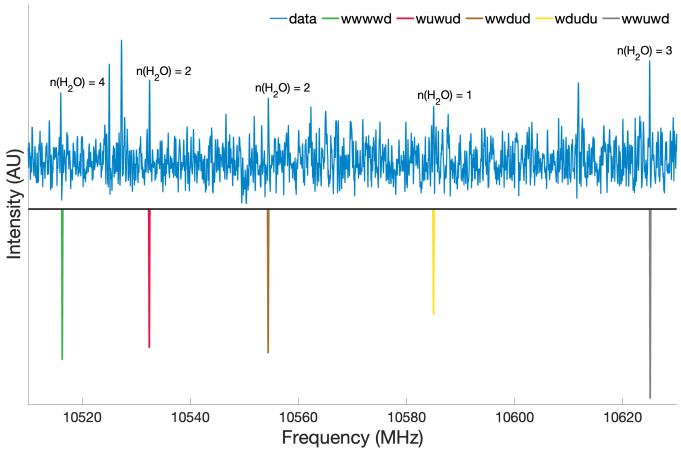

Fig. 4 Non-deuterated methanol:water spectrum from 10.51 – 10.63 GHz which encompasses experimentally observed lines for 1, 2, 3, and 4 water species. The SPCAT predicted lines below the data are generated using experimentally fitted constants. The experimentally observed pure methanol lines are all at higher frequencies.

Within each group of clusters (0, 1, 2, 3, or 4 waters) the conformers are close in energy, with the largest difference being less than 100 cm^{-1}. However, large energy gaps were calculated in the free energies from one group of clusters to another. This may be explained by the electron donating characteristics of the methyl group strengthening the ring of hydrogen bonding with higher methanol content, and the planar geometries that isolate the -CH_3 groups away from the H-bonded ring. Net cooperativity for all clusters remains two for each conformer studied here, since the cyclic hydrogen bonding scheme is unchanged, but as methanol is replaced with water, the bonds lengthen and the energy rises. The R_{O-O} distance for the pure water pentamer is 2.76 Å[35]. We find a steady decrease in bond length with additional methanol leading to pure methanol pentamer R_{O-O} distances averaging 2.71 Å. A lengthier analysis of R_{O-O} distances computationally, and supported with Kraitchman analysis experimentally, is left for the ESI.†

The abundance of each cluster across hydration levels depends on the experimental conditions, but the abundances of conformers *within* each hydration level can be used to constrain formation preferences in the molecular beam. To estimate relative abundances, we compared the ratios of SPCAT predicted intensity and experimental signal-to-noise for each peak used for fitting. The broadband nature and stability of the CP-FTMW instrument enables such measurements, especially when the lines are contained in a single LO setting. No significant difference in abundances between conformers was found for any of the hydration levels.

Clusters that contain two and three water monomers are where observations about a preference for homogeneous methanol and water mixing versus micro-aggregation could be made. All seven of the conformers at both hydration levels had similar relative abundances within error. However, the average root mean squared (rms) error of rotational constant fits for conformers

Ab Initio	wdudu	wuduu	wuudu	wduud	wudud
A /MHz	908.022	918.027	909.454	893.411	914.838
B /MHz	684.621	688.967	700.586	730.975	681.327
C /MHz	471.355	458.716	455.093	443.450	466.579
Δ_J /kHz	0.25	0.38	0.62	0.39	0.26
Δ_K /kHz	0.037	0.30	0.86	0.35	0.096
Δ_{JK} /kHz	-0.024	-0.48	-1.22	-0.61	-0.058
δ_J /kHz	0.028	0.022	0.020	0.012	0.032
δ_K /kHz	0.44	0.16	-0.020	-0.027	0.39
μ_a /D	0.21	-0.29	0.28	-0.14	-0.21
μ_b /D	-0.007	0.0007	-0.013	0.53	0.019
μ_c /D	-0.85	0.46	0.52	0.63	-0.89
Rel. Energy /cm^{-1}	0.0	20.0	33.4	37.6	55.1
Fitted	wdudu	wuduu	wuudu	wduud	wudud
A /MHz	908.112 (10)	917.911 (9)	909.342 (8)	893.433 (8)	914.852 (7)
B /MHz	684.615 (12)	688.970 (14)	700.493 (11)	731.018 (9)	681.325 (7)
C /MHz	471.365 (22)	458.761 (32)	455.035 (22)	443.407 (6)	466.618 (20)
Δ_J /kHz	0.35 (5)	0.44 (7)	0.20 (5)	0.75 (4)	0.43 (4)
Δ_K /kHz	1.86 (18)	0.31 (3)	0.46 (11)	1.74 (21)	0.91 (7)
Δ_{JK} /kHz	-1.64 (20)	-0.48	-1.04 (12)	-2.35 (25)	-0.82 (10)
δ_J /kHz	0.028	0.022	0.020	0.012 (1)	0.032
δ_K /kHz	1.11 (28)	0.16	-0.020	-1.14 (4)	0.39
μ_a /D	y	y	y	y	y
μ_b /D	n	n	n	y	n
μ_c /D	y	y	y	y	y
N	11	10	12	19	9
rms /kHz	52	53	125	71	60

Table 2 Calculated and experimental rotational constants for all conformers of $(H_2O)(CH_3OH)_4$. Fit with Watson's A-reduction. N is the number of lines from the experimental spectrum fit, and the values in parentheses are the errors reported by SPFIT. Experimental parameters shown without error were fixed to the computed values for fitting.

Ab Initio	wuwdu	wwudu	wuwuu	wwduu	wuwud	wwuud	wwdud
A /MHz	1214.986	1100.156	1201.816	1160.331	1225.138	1151.981	1079.695
B /MHz	764.841	841.598	781.493	829.540	754.099	846.101	856.745
C /MHz	521.846	560.856	519.499	533.594	517.083	526.792	573.945
Δ_J /kHz	0.54	0.85	0.67	0.73	0.45	0.84	0.72
Δ_K /kHz	0.14	2.18	-1.55	1.41	-0.19	1.45	1.49
Δ_{JK} /kHz	-0.48	-2.54	1.06	-1.85	-0.091	-2.12	-1.85
δ_J /kHz	0.060	0.15	0.11	0.10	0.075	0.044	0.08
δ_K /kHz	0.22	-1.75	2.17	-0.71	0.46	-0.85	-1.21
μ_a /D	0.18	0.16	-0.28	0.40	0.24	-0.38	-0.035
μ_b /D	0.13	-0.0059	-0.066	-0.30	0.21	-0.34	-0.080
μ_c /D	-0.72	0.76	0.40	0.48	0.68	0.58	-1.05
Rel. Energy /cm^{-1}	0.0	9.7	24.8	35.4	44.5	49.7	62.0
Fitted	wuwdu	wwudu	wuwuu	wwduu	wuwud	wwuud	wwdud
A /MHz	1214.916 (7)	1099.920 (21)	1201.801 (20)	1160.286 (10)	1225.010 (14)	1151.907 (5)	1079.444 (21)
B /MHz	764.938 (5)	841.911 (14)	781.473 (22)	829.637 (10)	754.200 (7)	844.562 (7)	856.775 (12)
C /MHz	521.844 (16)	561.918 (94)	519.612 (23)	533.481 (18)	517.079 (8)	526.623 (11)	573.119 (32)
Δ_J /kHz	0.48 (2)	0.78 (8)	0.45 (13)	0.33 (8)	0.49 (3)	0.091 (5)	0.36 (11)
Δ_K /kHz	0.14	0.012 (1)	-3.86 (5)	0.69 (18)	0.29 (3)	0.82 (11)	3.31 (4)
Δ_{JK} /kHz	-0.82 (5)	-2.54	2.93 (5)	-1.04 (21)	-0.091	-1.23 (15)	-5.56 (4)
δ_J /kHz	0.077 (6)	0.15	0.079 (9)	0.10	0.082 (15)	0.044	0.32 (3)
δ_K /kHz	0.44 (4)	-1.75	0.66 (5)	-0.71	0.38 (3)	-0.52 (7)	-3.37 (4)
μ_a /D	y	y	y	y	y	y	y
μ_b /D	n	n	n	y	y	y	n
μ_c /D	y	y	y	y	y	y	y
N	12	9	10	16	15	19	11
rms /kHz	87	151	82	66	18	87	56

Table 3 Calculated and experimental rotational constants for all conformers of $(H_2O)_2(CH_3OH)_3$. Fit with Watson's A-reduction. N is the number of lines from the experimental spectrum fit, and the values in parentheses are the errors reported by SPFIT. Experimental parameters shown without error were fixed to the computed values for fitting.

Ab Initio	wwdwu	wwwdd	wwuwu	wwwdu	wwuwd	wwwud	wwdwd
A /MHz	1729.155	1289.128	1663.684	1255.408	1737.443	1242.804	1630.047
B /MHz	862.093	1149.004	878.977	1153.530	866.887	1159.729	895.635
C /MHz	609.560	639.980	618.867	660.304	613.300	673.007	631.676
Δ_J /kHz	0.51	1.48	0.68	0.93	0.56	0.90	0.79
Δ_K /kHz	3.20	1.30	4.76	1.16	2.32	0.94	4.65
Δ_{JK} /kHz	-1.36	-2.59	-2.44	-1.60	-1.21	-1.51	-2.71
δ_J /kHz	-0.076	-0.067	-0.10	-0.044	-0.071	-0.0086	-0.13
δ_K /kHz	0.088	0.33	0.075	0.095	0.12	0.12	0.071
μ_a /D	-0.41	0.50	-0.19	-0.31	0.33	-0.0050	-0.15
μ_b /D	-0.078	0.0059	-0.21	-0.33	-0.18	-0.15	-0.10
μ_c /D	-0.76	0.45	0.63	0.81	-0.83	-0.92	0.65
Rel. Energy /cm^{-1}	0.0	1.50	51.6	59.7	65.5	66.8	95.5
Fitted	wwdwu	wwwdd	wwuwu	wwwdu	wwuwd	wwwud	wwdwd
A /MHz	1729.21 (15)	1289.22 (4)	1663.87 (14)	1255.47 (11)	1737.49 (15)	1243.09 (21)	1630.12 (14)
B /MHz	862.16 (12)	1148.91 (15)	879.09 (7)	1153.52 (8)	866.91 (6)	1159.51 (15)	895.69 (18)
C /MHz	609.08 (14)	640.05 (18)	618.61 (11)	660.34 (18)	613.25 (7)	673.07 (5)	631.73 (19)
Δ_J /kHz	0.57 (6)	3.11 (29)	1.77 (7)	1.18 (8)	0.81 (6)	0.90	1.42 (9)
Δ_K /kHz	2.54 (10)	7.02 (8)	6.19 (18)	1.16	1.71 (15)	0.94	3.22 (17)
Δ_{JK} /kHz	-0.83 (16)	-9.51 (10)	-5.77 (25)	-1.60	-1.00 (17)	-1.51	-2.06 (26)
δ_J /kHz	-0.18 (3)	-0.98 (14)	-0.45 (4)	-0.044	-0.27 (3)	-0.0086	-0.26 (3)
δ_K /kHz	0.40 (5)	16.8 (24)	1.06 (12)	0.095	0.49 (6)	0.12	0.67 (12)
μ_a /D	y	y	y	y	y	n	y
μ_b /D	n	n	y	y	y	y	n
μ_c /D	y	n	y	y	y	y	y
N	17	13	12	9	17	5	14
rms /kHz	93	66	58	169	64	131	61

Table 4 Calculated and experimental rotational constants for all conformers of $(H_2O)_3(CH_3OH)_2$. Fit with Watson's S-reduction. N is the number of lines from the experimental spectrum fit, and the values in parentheses are the errors reported by SPFIT. Experimental parameters shown without error were fixed to the computed values for fitting.

with micro-aggregated methanol and water clusters was 57% higher than for interspersed clusters. Taken together, these results imply no great preference in cluster formation between micro-aggregated structures and interspersed structures, though perhaps an increased difficulty in fitting structures with micro-aggregated methanol and water. This increased fitting error could be due to a number of causes – one explanation may lie in the large amplitude motion of these clusters. As internal rotation can split the rotational states, so too can the rotational spectrum be perturbed due to the large amplitude motion (LAM) of the underlying cluster geometry. Perhaps, in micro-aggregated water and methanol clusters, this LAM is more prevalent, or more impactful. Future high resolution studies would be beneficial in testing out this effect and conclusively determining the cause of the increased fitting error observed for micro-aggregated clusters. In addition, these future high resolution studies could fully fit the A-E splittings to probe large amplitude effects in different cluster conformers, determining whether any potential difference between aggregated and evenly dispersed clusters exists.

4 Conclusions

The aim of this chirped pulse rotational spectroscopy study was to survey the potential energy landscape of neat and mixed methanol and water pentamer conformers. From this work, the rotational constants and anharmonic corrections for 23 conformers have been fit from experimental data, guided by computational predictions. No clear distinction between micro-aggregated and interspersed conformers was observed, supporting the idea that methanol and water mix freely in small cluster topologies, where the effects of the methyl group are minimized.

In all of these clusters, a planar hydrogen bonding motif is observed, leading to a net cooperativity of two. Higher cooperativity clusters– i.e. clusters with a more 'three-dimensional' structure – were proposed, but were not found to be minima on the potential energy landscape for methanol and water pentamers. This result indicates that, for pentamers, a planar, ring-like structure remains lowest in energy, as has been the case for tetramers and trimers of mixed alcohol and water in previous studies. Building on this work, future experimentation will focus on hexamers. Water hexamers have been observed to be three-dimensional[36], breaking the net cooperativity of two trend we see in the pentamers, and showing promise for neat methanol or mixed methanol and water three dimensional hexamer clusters.

Author Contributions

We strongly encourage authors to include author contributions and recommend using CRediT for standardised contribution descriptions. Please refer to our general author guidelines for more information about authorship.

Conflicts of interest

There are no conflicts to declare.

Acknowledgements

The authors gratefully acknowledge support from the NSF CSDM-A program (Grant CHE-1665467) and the NASA Laboratory Astrophysics program (Grant NNX-16AC75G). SED is supported by the National Science Foundation Graduate Research Fellowship Program (Grant DGE-1745301). Any opinions, findings, and conclusions or recommendations expressed in this material are those of the authors and do not necessarily reflect the views of the National Science Foundation.

Ab Initio	wwwwu	wwwwd′	wwwwd
A /MHz	1976.914	1903.911	1946.883
B /MHz	1215.515	1254.966	1235.531
C /MHz	775.597	808.003	790.468
Δ_J /kHz	2.06	2.06	2.44
Δ_K /kHz	3.57	3.48	4.82
Δ_{JK} /kHz	-5.37	-5.18	-6.83
δ_J /kHz	0.49	0.36	0.51
δ_K /kHz	-2.38	-2.39	-3.47
μ_a /D	-0.42	0.048	-0.37
μ_b /D	0.022	0.051	0.12
μ_c /D	0.73	0.83	0.73
Rel. Energy /cm^{-1}	0.0	9.7	35.4
Fitted	wwwwu	wwwwd′	wwwwd
A /MHz	1976.920 (32)	1903.776 (18)	1946.976 (36)
B /MHz	1216.80 (39)	1255.018 (10)	1235.962 (45)
C /MHz	775.399 (70)	807.809 (13)	789.894 (66)
Δ_J /kHz	8.37 (19)	1.69 (7)	6.51 (6)
Δ_K /kHz	15.2 (35)	4.30 (11)	17.53 (19)
Δ_{JK} /kHz	-24.0 (55)	-5.18	-26.06 (28)
δ_J /kHz	5.08 (16)	0.36	1.33 (14)
δ_K /kHz	-12.3 (34)	-2.39	-3.96 (7)
μ_a /D	y	y	y
μ_b /D	n	y	n
μ_c /D	y	y	y
N	9	10	10
rms /kHz	82	44.7	7.2

Table 5 Calculated and experimental rotational constants for all conformers of $(H_2O)_4(CH_3OH)$. Fit with Watson's A-reduction. N is the number of lines from the experimental spectrum fit, and the values in parentheses are the errors reported by SPFIT. Experimental parameters shown without error were fixed to the computed values for fitting.

Notes and references

1 L. Pauling, R. B. Corey and H. R. Branson, *Proceedings of the National Academy of Sciences*, 1951, **37**, 205–211.

2 J. D. Watson and F. H. C. Crick, *Nature*, 1953, **171**, 737–738.

3 H. Zhao, S. Tang, X. Xu and L. Du, *International Journal of Molecular Sciences*, 2016, **18**, 4.

4 *Hydrogen bonding: new insights*, ed. S. J. Grabowski, Springer, Dordrecht, 2006.

5 D. Patkar, M. B. Ahirwar and M. M. Deshmukh, *ChemPhysChem*, 2022, **23**, e202200143.

6 R. Ludwig, *Angewandte Chemie International Edition*, 2001, **40**, 1808–1827.

7 W. Li, C. Pérez, A. L. Steber, M. Schnell, D. Lv, G. Wang, X. Zeng and M. Zhou, *Journal of the American Chemical Society*, 2023, **145**, 4119–4128.

8 A. L. Steber, B. Temelso, Z. Kisiel, M. Schnell and C. Pérez, *Proceedings of the National Academy of Sciences*, 2023, **120**, e2214970120.

9 W. Roth, M. Schmitt, C. Jacoby, D. Spangenberg, C. Janzen and K. Kleinermanns, 1998.

10 N. Guchhait, T. Ebata and N. Mikami, *The Journal of Chemical Physics*, 1999, **111**, 8438–8447.

11 U. Buck and F. Huisken, *Chemical Reviews*, 2000, **100**, 3863–3890.

12 Y.-F. Lee, A.-M. Kelterer, G. Matisz, S. Kunsági-Máté, C.-Y. Chung and Y.-P. Lee, *The Journal of Chemical Physics*, 2017, **146**, 144308.

13 M. Nedić, T. N. Wassermann, R. W. Larsen and M. A. Suhm, *Physical Chemistry Chemical Physics*, 2011, **13**, 14050.

14 O. Kostko, L. Belau, K. R. Wilson and M. Ahmed, *The Journal of Physical Chemistry A*, 2008, **112**, 9555–9562.

15 A. Mandal, M. Prakash, R. M. Kumar, R. Parthasarathi and V. Subramanian, *The Journal of Physical Chemistry A*, 2010, **114**, 2250–2258.

16 M. Haughney, M. Ferrario and I. R. McDonald, *The Journal of Physical Chemistry*, 1987, **91**, 4934–4940.

17 A. Mellouki, T. J. Wallington and J. Chen, *Chemical Reviews*, 2015, **115**, 3984–4014.

18 Z. Li, Y. Wang, Z. Yin, Z. Gao, Y. Wang and X. Zhen, *Fuel*, 2021, **304**, 121466.

19 H. Sun, W. Wang and K.-P. Koo, *International Journal of Engine Research*, 2019, **20**, 350–358.

20 G. A. Olah, *Angewandte Chemie International Edition*, 2005, **44**, 2636–2639.

21 A. V. Shindyapina, I. V. Petrunia, T. V. Komarova, E. V. Sheshukova, V. S. Kosorukov, G. I. Kiryanov and Y. L. Dorokhov, *PLoS ONE*, 2014, **9**, e102837.

22 Y. L. Dorokhov, A. V. Shindyapina, E. V. Sheshukova and T. V. Komarova, *Physiological Reviews*, 2015, **95**, 603–644.

23 S. E. Dutton and G. A. Blake, *Physical Chemistry Chemical Physics*, 2022, **24**, 13831–13838.

24 P. A. Stockman, G. A. Blake, F. J. Lovas and R. D. Suenram, *The Journal of Chemical Physics*, 1997, **107**, 3782–3790.

25 L. González, O. Mó and M. Yáñez, *The Journal of Chemical Physics*, 1998, **109**, 139–150.

26 J. L. Iosue, D. M. Benoit and D. C. Clary, *Chemical Physics Letters*, 1999, **301**, 275–280.

27 I. A. Finneran, P. B. Carroll, M. A. Allodi and G. A. Blake, *Physical Chemistry Chemical Physics*, 2015, **17**, 24210–24214.

28 S. E. Dutton, E. M. Mastin and G. A. Blake, *Physical Chemistry Chemical Physics*, 2023, **25**, 5960–5966.

29 M. J. Frisch, G. W. Trucks, H. B. Schlegel, G. E. Scuseria, M. A. Robb, J. R. Cheeseman, G. Scalmani, V. Barone, G. A. Petersson, H. Nakatsuji, X. Li, M. Caricato, A. V. Marenich, J. Bloino, B. G. Janesko, R. Gomperts, B. Mennucci, H. P. Hratchian, J. V. Ortiz, A. F. Izmaylov, J. L. Sonnenberg, D. Williams-Young, F. Ding, F. Lipparini, F. Egidi, J. Goings, B. Peng, A. Petrone, T. Henderson, D. Ranasinghe, V. G. Zakrzewski, J. Gao, N. Rega, G. Zheng, W. Liang, M. Hada, M. Ehara, K. Toyota, R. Fukuda, J. Hasegawa, M. Ishida, T. Nakajima, Y. Honda, O. Kitao, H. Nakai, T. Vreven, K. Throssell, J. A. Montgomery, Jr., J. E. Peralta, F. Ogliaro, M. J. Bearpark, J. J. Heyd, E. N. Brothers, K. N. Kudin, V. N. Staroverov, T. A. Keith, R. Kobayashi, J. Normand, K. Raghavachari, A. P. Rendell, J. C. Burant, S. S. Iyengar, J. Tomasi, M. Cossi, J. M. Millam, M. Klene, C. Adamo, R. Cammi, J. W. Ochterski, R. L. Martin, K. Morokuma, O. Farkas, J. B. Foresman and D. J. Fox, *Gaussian~16 Revision C.01*, 2016, Gaussian Inc. Wallingford CT.

30 C. M. Western, *Journal of Quantitative Spectroscopy and Radiative Transfer*, 2017, **186**, 221–242.

31 H. PICKETT, R. POYNTER, E. COHEN, M. DELITSKY, J. PEAR-

SON and H. MÜLLER, *Journal of Quantitative Spectroscopy and Radiative Transfer*, 1998, **60**, 883–890.

32 H. Hartwig and H. Dreizler, *Zeitschrift für Naturforschung A*, 1996, **51**, 923–932.

33 K. Liu, J. D. Cruzan and R. J. Saykally, *Science*, 1996, **271**, 929–933.

34 C. Puzzarini, J. F. Stanton and J. Gauss, *International Reviews in Physical Chemistry*, 2010, **29**, 273–367.

35 K. Liu, M. G. Brown, J. D. Cruzan and R. J. Saykally, *The Journal of Physical Chemistry A*, 1997, **101**, 9011–9021.

36 C. Pérez, M. T. Muckle, D. P. Zaleski, N. A. Seifert, B. Temelso, G. C. Shields, Z. Kisiel and B. H. Pate, *Science*, 2012, **336**, 897–901.